Time-fractional heat conduction law in a magneto-thermoelastic solid with hydrostatic initial stress

Nantu Sarkar [a] *,

[a] Department of Applied Mathematics, University of Calcutta, Kolkata-700 009, India.

ABSTRACT

In this paper, the theory of fractional order two-temperature generalized thermoelasticity is used to study the propagation of magneto-thermoelastic disturbances in a homogeneous isotropic perfectly conducting half-space medium due hydrostatic initial stress. Normal mode analysis technique and the method of displacement potentials are used to obtain the analytical solutions of the studied field varables. Arbitrary application is chosen to enable us to get the complete solution. The effect of fractional parameter and hydrostatic initial stress on the variations of the studied field quantities has been investigated graphically.

1. Introduction

Several investigations have been made by many authors using the fractional calculus to study the physical processes. Ezzat and Karmany [1] applied the new Taylor series expansion of time-fractional order which was developed in [2] based on the classical Fourier heat conduction law to establish fractional order heat conduction law in magneto-thermoelasticity involving two temperatures. They studied a one-dimensional problem for a thermoelastic medium of prefect conductivity permeated by an initial magnetic field using the above fractional order generalized thermoelasticity model and investigated the effects of the fractional order parameter on all the studied physical quantities in the same work.

The effects of fractional parameter on the plane waves of generalized magneto - thermoelastic diffusion with reference temperature-dependent elastic medium by Othman et al. [3]. Abbas [4] investigated a problem on functional graded material within the framework of fractional generalized thermoelasticity.Youssef [5] studied a one-dimensional problem in the context of the fractional order generalized thermoelasticity. Povstenko in-

*Email : nsappmath@caluniv.ac.in

troduced a new fractional heat conduction equation and studied associated thermal stress in [6]. Povstenko [7] also investigated the fractional radial diffusion in an infinite medium with cylindrical cavity. Bachher et al. [8, 9] studied some one-dimensional thermoelastic problems for infinite porous material with heat sources in the context of the fractional order generalized thermoelasticity theorey.

In the present work, the theory of fractional order two-temperature generalized thermoelasticity is applied to study the propagation of magneto-thermoelastic disturbances in a homogeneous isotropic perfectly conducting half-space medium due hydrostatic initial stress. Normal mode analysis [10-12] technique and the method of displacement potentials [3] are used to obtain the analytical solutions of the studied field varables. Arbitrary application is chosen to enable us to get the complete solution. The effect of fractional parameter and hydrostatic initial stress on the variations of the studied field quantities has been investigated graphically.

2. Formulation of the problem

We shall consider a homogeneous isotropic perfectly conducting thermoelastic semi-infinite medium ($x \geq 0$) with hydrostatic initial stress in two-dimensional space under constant primary magnetic field $\vec{H}_0 = (0, 0, H_0)$ acts parallel to the boundary plane (taken as the direction of the z-axis). This produces an induced magnetic field $\vec{h} = (0, 0, h_0)$ and induced electric field $\vec{E} = (E_1, E_2, 0)$ which satisfy the linearized equations of electromagnetism and are valid for slowly moving media : [3] :

$$\vec{J} = \vec{\nabla} \times \vec{h} - \varepsilon_0 \dot{\vec{E}} \tag{1}$$

$$\vec{\nabla} \times \vec{E} = -\mu_0 \dot{\vec{h}} \tag{2}$$

$$\vec{E} = -\mu_0 \left(\dot{\vec{u}} \times \vec{H} \right) \tag{3}$$

$$\vec{\nabla} \cdot \vec{h} = 0, \ \vec{\nabla} \cdot \vec{E} = 0 \tag{4}$$

where $\vec{H} = \vec{H}_0 + \vec{h}$,is the total magnetic field vector, $\vec{J}$ is the electric current density, ε_0 is the electric permeability and μ_0 is the magnetic permeability.

The above equations are supplemented by the governing equations of linear, homogenous and isotropic fractional order generalized magneto-thermoelasticity with hydrostatic initial stress (Lord and Shulman [13], Montanaro [14], Youssef [15], and Ezzat and Karamany [1]) as follows :

$$\sigma_{ij} = -p \left(\delta_{ij} + \omega_{ij} \right) + 2\mu e_{ij} + \left(\lambda e_{kk} - \gamma \theta \right) \delta_{ij} \tag{5}$$

$$e_{ij} = \frac{1}{2} \left(u_{i,j} + u_{j,i} \right) \tag{6}$$

$$\omega_{ij} = \frac{1}{2}\left(u_{j,i} - u_{i,j}\right) \tag{7}$$

$$\sigma_{ij,j} + \mu_0\left(\vec{J} \times \vec{H}\right)_i = \rho \ddot{u}_i \tag{8}$$

$$k\nabla^2\theta = \frac{\partial}{\partial t}\left(1 + \frac{\tau_0^\alpha}{\alpha!}\frac{\partial^\alpha}{\partial t^\alpha}\right)\left(\rho C_E \theta + \gamma T_0 e\right), \ 0 < \alpha \le 1 \tag{9}$$

where σ_{ij} are the components of the stress tensor, e_{ij} are the components of strain tensor, u_i are the components of the displacement vector $\vec{u}$, λ, μ are the counterparts of Lame's constants, $\gamma = (3\lambda + 2\mu)\alpha_T$ is a material constant characteristic of the theory, α_T is the coefficient of linear thermal expansion, δ_{ij} is Kronecker delta, p is the initial pressure, ω_{ij} are the components of the small rotation tensor, ρ is the mass density, $k(> 0)$ is the thermal conductivity, C_E is the specific heat at constant strain, $\theta = T - T_0$ is small temperature increment, T is the temperature increase of the medium over the uniform reference temperature T_0 assumed to be such that $|\theta/T_0| << 1$, $e = e_{kk}$ is the cubical dilatation and $a(> 0)$ is the temperature discrepancy. In the above equations, the comma notation is used for derivatives with respect to space variables and superimposed dot represents time differentiation.

For two-dimensional deformation in the xy-plane, all the considered functions will depend on space variables x, y and time variable t and thus the displacement vector $\vec{u}$ will have the components :

$$u = u_x = u(x,y,t), \ v = u_y = v(x,y,t), \ w = u_z = 0. \tag{10}$$

Eqs. (1)-(9) thus simplify to :

$$\sigma_{xx} = \left(\lambda + 2\mu\right)u_{,x} + \lambda\,v_{,y} - \gamma\theta - p \tag{11}$$

$$\sigma_{yy} = \lambda u_{,x} + \left(\lambda + 2\mu\right)v_{,y} - \gamma\theta - p \tag{12}$$

$$\sigma_{xy} = \left(\mu - \frac{p}{2}\right)v_{,x} + \left(\mu + \frac{p}{2}\right)u_{,y} \tag{13}$$

$$\sigma_{yx} = \left(\mu + \frac{p}{2}\right)v_{,x} + \left(\mu - \frac{p}{2}\right)u_{,y} \tag{14}$$

$$\left(\lambda + 2\mu + \mu_0 H_0^2\right)u_{,xx} + \left(\lambda + \mu + \frac{p}{2} + \mu_0 H_0^2\right)v_{,xy} + \left(\mu - \frac{p}{2}\right)u_{,yy} - \gamma\theta_{,x} = \rho\left(1 + \varepsilon_0\mu_0^2 H_0^2\right)\ddot{u} \tag{15}$$

$$\left(\lambda + 2\mu + \mu_0 H_0^2\right) v_{,yy} + \left(\lambda + \mu + \frac{p}{2} + \mu_0 H_0^2\right) u_{,xy} + \left(\mu - \frac{p}{2}\right) v_{,xx} - \gamma \theta_{,y} = \rho \left(1 + \varepsilon_0 \mu_0^2 H_0^2\right) \ddot{v} \tag{16}$$

For the purpose of numerical evaluation, we will use the following non-dimensional variables

$$(x', y', u', v') = c_1 \eta(x, y, u, v), \ (t', \tau_0') = c_1^2 \eta(t, \tau_0),$$

$$\sigma'_{ij} = \frac{\sigma_{ij}}{\rho c_1^2}, \ \theta' = \frac{\gamma}{\rho c_1^2} \theta, p' = \frac{p}{\rho c_1^2}, \ \eta = \frac{\rho C_E}{k} \tag{17}$$

Using the above non-dimensional variables, Eqs. (11)-(16), (8) and (9) take the following forms (omitting the primes for convenience) :

$$\sigma_{xx} = u_{,x} + \left(1 - 2\beta^2\right) v_{,y} - \theta - p \tag{18}$$

$$\sigma_{yy} = v_{,y} + \left(1 - 2\beta^2\right) u_{,x} - \theta - p \tag{19}$$

$$\sigma_{xy} = \left(\beta^2 - \frac{p}{2}\right) v_{,x} + \left(\beta^2 + \frac{p}{2}\right) u_{,y} \tag{20}$$

$$\sigma_{yx} = \left(\beta^2 + \frac{p}{2}\right) v_{,x} + \left(\beta^2 - \frac{p}{2}\right) u_{,y} \tag{21}$$

$$\left(1 + c_3^2\right) u_{,xx} + \left(1 - \beta^2 + \frac{p}{2} + c_3^2\right) v_{,xy} + \left(\beta^2 - \frac{p}{2}\right) u_{,yy} - \left(1 - \beta_0 \nabla^2\right) \varphi_{,x} = M\ddot{u} \tag{22}$$

$$\left(1 + c_3^2\right) v_{,yy} + \left(1 - \beta^2 + \frac{p}{2} + c_3^2\right) u_{,xy} + \left(\beta^2 - \frac{p}{2}\right) v_{,xx} - \left(1 - \beta_0 \nabla^2\right) \varphi_{,y} = M\ddot{v} \tag{23}$$

$$\nabla^2 \theta = \frac{\partial}{\partial t} \left(1 + \frac{\tau_0^\alpha}{\alpha!} \frac{\partial^\alpha}{\partial t^\alpha}\right) (\theta + \varepsilon e) \tag{24}$$

$$e = (u_{,x} + v_{,y}) \tag{25}$$

where $\beta^2 = \frac{\mu}{\lambda + 2\mu}, \ \varepsilon = \frac{\gamma^2 T_0}{\rho C_E (\lambda + 2\mu)}, \ c_3^2 = \frac{\mu_0 H_0^2}{\lambda + 2\mu}, \ M = \left(1 + \varepsilon_0 \mu_0^2 H_0^2\right).$

We define the displacement potentials and which relate to displacement components u and ν as

$$u = \vartheta_{,x} + \psi_{,y}, \ v = \vartheta_{,y} - \psi_{,x} \tag{26}$$

so that

$$e = \nabla^2 \vartheta \tag{27}$$

Using Eq. (25) and (26) in Eqs. (21)-(23), we obtain :

$$\left[\left(1 + c_3^2 \right) \nabla^2 - M \frac{\partial^2}{\partial t^2} \right] \vartheta - \theta = 0, \tag{28}$$

$$\left[\left(\beta^2 - \frac{p}{2} \right) \nabla^2 - M \frac{\partial^2}{\partial t^2} \right] \psi = 0, \tag{29}$$

$$\left[\nabla^2 - \frac{\partial}{\partial t} \left(1 + \frac{\tau_0^\alpha}{\alpha!} \frac{\partial^\alpha}{\partial t^\alpha} \right) \right] \theta - \varepsilon \frac{\partial}{\partial t} \left(1 + \frac{\tau_0^\alpha}{\alpha!} \frac{\partial^\alpha}{\partial t^\alpha} \right) \nabla^2 \vartheta = 0. \tag{30}$$

3. Normal mode analysis

The solution of the physical quantities can be decomposed in terms of normal modes in the following form :

$$[\vartheta, \psi, \theta] \, (x.y.t) = [\vartheta^*, \psi^*, \theta^*] \, (x) e^{\omega t + imy}, \tag{31}$$

where $\vartheta^*(x)$ etc. are the amplitude of the function $\vartheta(x, y, t)$ etc., i is the imaginary unit, ω is the angular frequency and m is the wave number in the y-direction.

Introducing (30) in Eqs. (27)-(29), we obtain

$$\left[\left(1 + c_3^2 \right) \left(D^2 - m^2 \right) - M \omega^2 \right] \vartheta^* - \theta^* = 0 \tag{32}$$

$$\left[\left(\beta^2 - \frac{p}{2} \right) \left(D^2 - m^2 \right) - M \omega^2 \right] \psi^* = 0 \tag{33}$$

$$\left[\left(D^2 - m^2 \right) - \omega_0 \right] \theta^* - \varepsilon \omega_0 \left(D^2 - m^2 \right) \vartheta^* = 0 \tag{34}$$

where

$$\omega_0 = \omega \left(1 + \frac{\tau_0^\alpha}{\alpha!} e^{-\omega t} t^{-\alpha} \sum_{n=1}^{\infty} \frac{(\omega t)^n}{\Gamma(n + 1 - \alpha)} \right) \tag{35}$$

Eliminating $\vartheta^*(x)$ and $\theta^*(x)$ from Eqs. (31) and (33), we get the following fourth-order ordinary differential equation satisfied by $\vartheta^*(x)$ and $\theta^*(x)$.

$$\left(D^4 - A D^2 + B \right) \{ \vartheta^*(x), \theta^*(x) \} = 0$$

where $A = 2m^2 + g_1, \quad B = m^4 + g_1 m^2 + g_2,$

$g_1 = [\omega_0 \left(1 + c_3^2 \right) + M \omega^2 + \varepsilon \omega_0] \left[(1 + c_3^2) + \varepsilon \beta_0 \omega_0 \right]^{-1}, g_2 = M \omega_0 \omega^2 [(1 + c_3^2) + \varepsilon \beta_0 \omega_0]^{-1}.$

Eq. (35) can be factorized as

$$\left(D^2 - k_1^2 \right) \left(D^2 - k_2^2 \right) \{ \vartheta^*(x), \theta^*(x) \} = 0 \tag{36}$$

where k_j $[\text{Re}\,(k_j) > 0, \; j = 1, 2]$ are the roots of the following characteristic equation.

$$k^4 - g_1 k^2 + g_2 = 0 \tag{37}$$

given by $k_1^2, \; k_2^2 = \frac{g_1 \pm \sqrt{g_1^2 - 4g_2}}{2}$.

The general solution for $\vartheta^*(x)$, $\psi^*(x)$ and $\theta^*(x)$ which are bounded as $x \to +\infty$ can be written from Eqs. (32) and (36) as

$$\vartheta^*(x) = \sum_{j=1}^{2} R_j e^{-k_j x} \tag{38}$$

$$\psi^*(x) = R_3 e^{-k_3 x} \tag{39}$$

$$\theta^*(x) = \sum_{j=1}^{2} \delta_j R_j e^{-k_j x} \tag{40}$$

where R_j $(j = 1, 2, 3)$ are some parameters depending on m, ω
and $k_3 = \sqrt{m^2 + M\omega^2 \left(\beta^2 - \frac{p}{2}\right)^{-1}}(> 0)$, $\delta_j = \left[(1 + c_3^2)\left(k_j^2 - m^2\right) - M\omega^2\right]$, $j = 1, 2$.
Using Eqs. (30), (38) and (39) in Eqs (25) and (26), the solutions for the strain $e(x, y, t)$ and the displacements components $u(x, y, t)$ and $v(x, y, t)$ can now be obtained as

$$e(x, y, t) = e^{\omega t + imy} \sum_{j=1}^{2} \left(k_j^2 - m^2\right) R_j e^{-k_j x} \tag{41}$$

$$u(x, y, t) = e^{\omega t + imy} \left[imR_3 e^{-k_3 x} - \sum_{j=1}^{2} k_j R_j e^{-k_j x}\right] \tag{42}$$

$$v(x, y, t) = e^{\omega t + imy} \left[k_3 R_3 e^{-k_3 x} + \sum_{j=1}^{2} imR_j e^{-k_j x}\right] \tag{43}$$

Substituting from Eqs. (40), (42) and (43) into the Eqs. (17)-(20), we get the following expressions for the stress components

$$\sigma_{xx}(x, y, t) = -p + e^{\omega t + imy} \sum_{j=1}^{3} \delta_{2j} R_j e^{-k_j x} \tag{44}$$

$$\sigma_{yy}(x, y, t) = -p + e^{\omega t + imy} \sum_{j=1}^{3} \delta_{3j} R_j e^{-k_j x} \tag{45}$$

$$\sigma_{xy}(x,y,t) = e^{\omega t+imy}\sum_{j=1}^{3}\delta_{4j}R_{j}e^{-k_{j}x} \tag{46}$$

$$\sigma_{yx}(x,y,t) = e^{\omega t+imy}\left[\sum_{j=1}^{2}\delta_{4j}R_{j}e^{-k_{j}x} + \delta_{44}R_{3}e^{-k_{3}x}\right] \tag{47}$$

where
$\delta_{2j} = \left[\left(k_{j}^{2}-m^{2}\right)+2m^{2}\beta^{2}-1\right],\ \delta_{23} = -2im\beta^{2}k_{3},$
$\delta_{3j} = \left[\left(k_{j}^{2}-m^{2}\right)-2k_{j}^{2}\beta^{2}-1\right],\ \delta_{33} = 2im\beta^{2}k_{3},$
$\delta_{4j} = -2im\beta^{2}k_{j},$
$\delta_{4j+2} = (-1)^{j-1}\frac{p}{2}\left(k_{3}^{2}-m^{2}\right)-\beta^{2}\left(k_{3}^{2}+m^{2}\right),\ \ j=1,2.$

4. Application

We consider the problem of a fractional order magneto-thermoelastic semi-infinite medium Ω with hydrostatic initial stress and two-temperature defined as follows :

$$\Omega = \{(x,y,z): 0 \leq x < \infty,\ -\infty < y < \infty,\ -\infty < z < \infty\}.$$

We assume the following initial conditions :

$$u = v = \theta = \varphi = \dot{u} = \dot{v} = \dot{\theta} = \dot{\varphi} = 0 \ \text{at}\ t = 0. \tag{48}$$

We now apply the following boundary conditions for the present problem :
(i) Thermal boundary condition : the surface $x = 0$ is assumed to be thermally insulated i.e.,

$$\frac{\partial\theta}{\partial x} = 0, \text{on } x = 0 \tag{49}$$

(ii) Mechanical boundary condition : the boundary conditions for a load p_0 applied at the plane surface $x = 0$ of the medium Ω in normal direction can be mathematically written as

$$\sigma_{xx}(0,y,t) = -p_0,\ \sigma_{xy}(0,y,t) = 0 \tag{50}$$

Substituting the expressions of the variables considered into the above boundary conditions, we obtain the following equations satisfied by the parameters R_j $(j = 1, 2, 3)$.

$$g_{11}R_1 + g_{12}R_2 = 0$$

$$\delta_{21}R_1 + \delta_{22}R_2 + \delta_{23}R_3 = p^{*}$$

$$\delta_{41}R_1 + \delta_{42}R_2 + \delta_{43}R_3 = 0$$

where $g_{1j} = (\kappa - k_j)\,\delta_j$, $p^* = (p - p_0)\,e^{-\omega t - imy}$.
Solving Eqs. (51)-(53), we get the parameters R_j $(j = 1, 2, 3)$ with the following forms :

$$R_1 = \frac{-p^* g_{12} \delta_{43}}{\Delta}\,,\ R_2 = \frac{p^* g_{11} \delta_{43}}{\Delta}\,, R_3 = \frac{p^* (g_{12} \delta_{41} - g_{11} \delta_{42})}{\Delta} \tag{51}$$

where $\Delta = g_{11} (\delta_{22} \delta_{43} - \delta_{23} \delta_{42}) - g_{12} (\delta_{21} \delta_{43} - \delta_{23} \delta_{41})\,.$

5. Special cases of thermoelasticity theory

5.1. Classical dynamical theory of thermoelasticity (CD theory)
Setting $\alpha = 1$ and $\tau_0 = 0$, the equations of the CD-theory can be obtained.

5.2. Lord-Shulman theory of thermoelasticity (L-S model)
Setting $\alpha = 1$ where $\tau_0 > 0$, the equations of the L-S theory can be obtained.

5.3. Fractional order theory of generalized thermoelasticity
In this case, $0 < \alpha < 1$ with $\tau_0 > 0$.

6. Particular cases

6.1. Fractional order generalized thermoelastic medium with hydrostatic initial stress ;
Substitutin $H_0 = 0$ in Eqs. (17)-(24), we obtain the corresponding expressions of all the physical quantities.

6.2. Fractional order generalized magneto-thermoelasticity without hydrostatic initial stress ;
Setting $p = 0$ in Eqs. (17)-(24), we obtain the corresponding expressions of all the physical quantities.

6.3. Fractional order generalized thermoelasticity without hydrostatic initial stress and magnetic field ;
Substituting $H_0 = 0$ and $p = 0$ in Eqs. (17)-(24) we can obtain the corresponding expressions of the temperature, the displacements and the stress distributions.

7. Numerical results

In order to illustrate the effects of the fractional parameter, two-temperature parameter, initial stress on the field variables, a numerical analysis is presented. Material chosen for this purpose is magnesium crystal, the physical data for which is given in Table 1 [9].

Table 1 – Physical data for magnesium crystal.

$\rho = 1.74 \times 10^3 \,\text{kgm}^{-3}$	$\mu = 3.278 \times 10^{10}\text{Nm}^{-2}$	$\lambda = 2.17 \times 10^{10}\text{Nm}^{-2}$
$k = 1.7 \times 10^2 \text{Wm}^{-1}\text{K}^{-1}$	$C_E = 1.04 \times 10^2 \text{Jkg}^{-1}\text{deg}^{-1}$	$\varepsilon_0 = \frac{10^{-9}}{36\pi}\text{Fm}^{-1}$
$H_0 = \frac{10^7}{4\pi}\text{Am}^{-1}$	$T_0 = 298\,\text{K}$	$\tau_0 = 0.02$
$m = 4.0$	$p_0 = 1$	$\kappa = 0$
$\gamma = 2.68 \times 10^6 \,\text{Nm}^{-2}\text{deg}^{-1}$	$\mu_0 = \frac{4\pi}{10^7}\text{Hm}^{-1}$	$\omega = 3.0$

Using the above data, the value of the series (34) has been computed and on a personal computer with the help of Mathematica software and the values are noted in Table 2 :

Table 2 – Value of the series (34).

α	0.1	0.5	1.0
ω_0	5.59037	4.09827	3.18

Considering the above physical data, the real parts of the non-dimensional physical variables have been computed and the obtained numerical values are presented in the form of graphs at different positions of the distance x at $t = 0.3$ and $y = 0.0$. We have plotted two sets of graphs. The first sets of graphs (Figs. 1-6) show the effect of the fractional parameter $\alpha = 0.1$, 0.5, 1.0 on the distribution of the field variables. The variation of the field variables due to hydrostatic initial stress $p = 0.0$, 0.2, 0.4 has been depicted in the second set of figures (Figs. 7– 12). All the figures in second set are shown for $\alpha = 0.5$.

Figs. 1 and 2 depict the variations of the temperature θ and the strain field e at different positions of x for three different values of $\alpha = 0.1$, 0.5, 1.0 and $\beta_0 = 0.1$, $p = 5.0$. From this figure, we can notice that both the field variables have similar behavior qualitatively having some difference in magnitudes only. However, for large value of α, magnitudes of both the temperature and strain fields are larger as compared to the case when $\alpha = 0.1$ which clearly indicates that the fractional parameter α has an increasing effect on θ and e. When the free surface of the half-space is affected by the external load, the temperature rise velocity becomes very fast, causing the temperature gradient to increase dramatically. As a result, temperature fields attain their peak values near the boundary. As the horizontal distance x increases, the temperature rise velocity and the temperature gradient decrease, so the temperature fields weaken to a comparatively small value and ultimately reach to steady state for $x \geq 3.5$ (approximately). Thus, it can be seen that the thermodynamics is a short time effect.
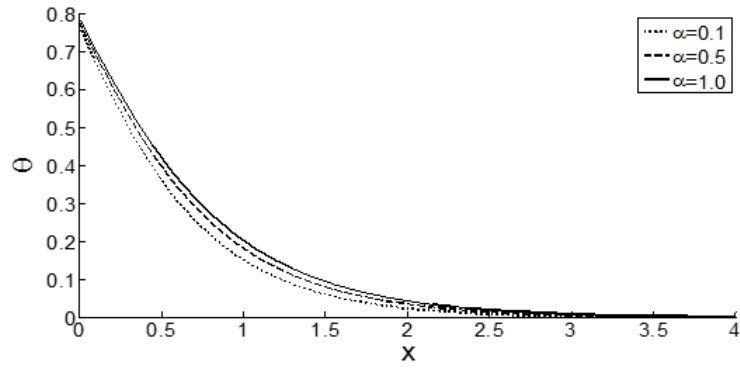
Fig. 1 – Temperature distribution for $p = 5.0$.
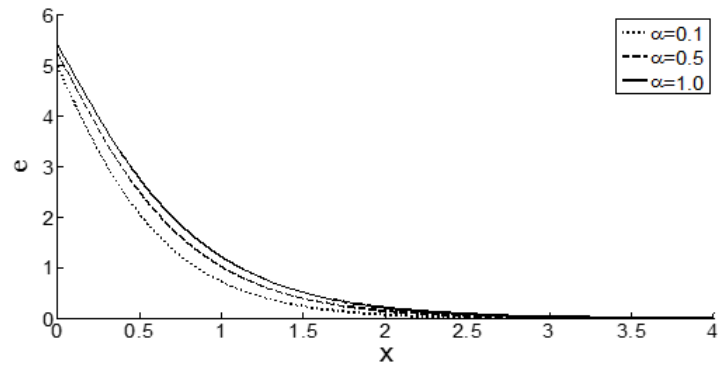
Fig. 2 – Distribution of the strain field for $p = 5.0$.
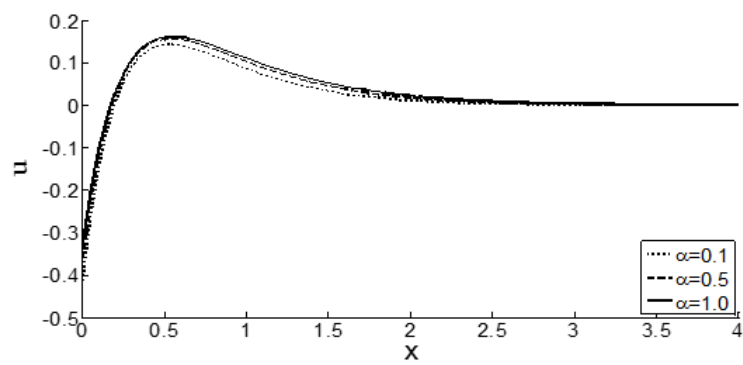
Fig. 3 – Horizontal displacement distribution for $p = 5.0$.

Fig. 3 displays the spatial variation of the horizontal displacement u with respect to x $(0.0 \leq x \leq 4.0)$ at $\alpha = 0.1$, 0.5, 1.0, $\beta_0 = 0.1$, $p = 5.0$. This figure indicates that u

starts with the positive value 0.049 (approximately) in all the three cases, then it starts to increase and attains stationary maximum value (+ve) at $x = 0.47$ (approximately) for $\alpha = 0.1$. After reaching the maximum value, the displacement starts to decrease as the distance x increases and at last becomes zero at the heat wave front. Effect of the fractional parameter α is quite pertinent on the distributions of u which can be easily noticed from the figure. Increment in the value of α has caused decrement in the numerical value of u within the region $0.0 \leq x \leq 0.47$ and then α acts to increase the magnitudes of u in $0.47 \leq x \leq 4.0$.

Distribution of the non-dimensional normal stress components σ_{xx} and σ_{yy} with spatial coordinate x has been plotted in Fig. 4 and 5 for $\alpha = 0.1, 0.5, 1.0$ and $\beta_0 = 0.1$, $p = 5.0$. Fig. 4 shows that in all the three cases, σ_{xx} starts with a negative value -1.0 which is completely in agreement with the boundary conditions (50) and then it is decreasing for $0.0 \leq x \leq 3.5$. The stress σ_{xx} converges to the value -5.0 for $x \geq 3.5$ which is again agrees with our theoretical results (44) because for large value of $x \geq 3.5$, the second term of σ_{xx} in Eq. (44) converges to zero value and hence $\sigma_{xx} \simeq -5.0$ for $x \geq 3.5$. The vibration amplitude quickly rises to its maximum value near the boundary of the surface which is called the peak deflection. Similar behavior of the other normal stress component σ_{yy} has been found in Fig. 5. Figs. 4 and 5 illuminates that the fractional parameter is having a significant decreasing effect on the profile of both the normal stress distributions.

Fig. 6 represents the distribution of the non-dimensional shearing stress component σ_{xy} vs. x for three different value of the fractional parameter $\alpha = 0.1, 0.5, 1.0$ and indicates that σ_{xy} starts with a zero value for all the three cases which agrees with the assumed boundary condition (50). Hence the numerical results agree with our theoretical results. The parameter α acts to decrease the values σ_{xy} of in the region $0.0 \leq x \leq 0.4$ (approximately) and then increases further to reach its steady state. It can be noticed that the maximum impact zone of α is $0.0 \leq x \leq 3.5$ (approximately) and this impact dies outside this range. Stress field attains significantly large values in for small value of $\alpha = 0.1$ compared to $\alpha = 0.5, 1.0$. This figure also shows that σ_{xy} attains two extreme values-one is maximum value and the other is a minimum value.
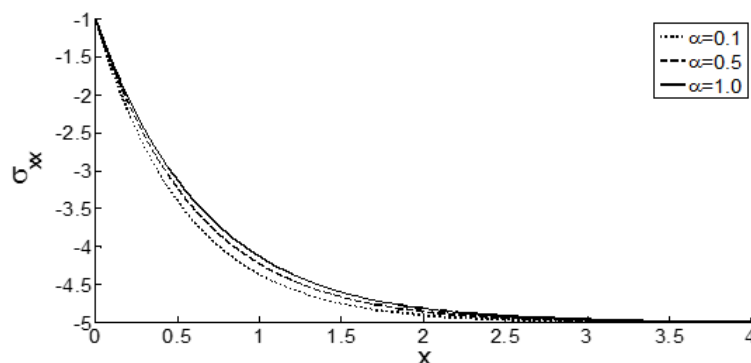
Fig. 4 – Distribution of the normal stress σ_{xx} for $p = 5.0$.
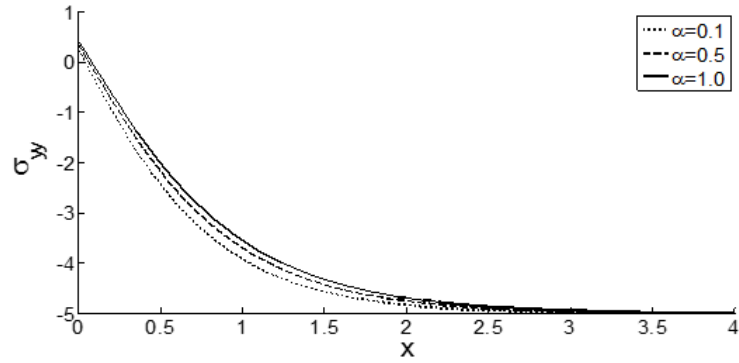
Fig. 5 – Distribution of the normal stress σ_{yy} for $p = 5.0$.
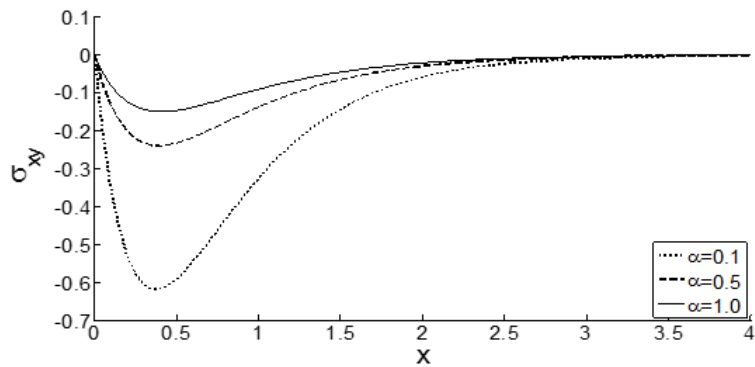
Fig. 6 – Distribution of the shearing stress σ_{xy} for $p = 5.0$.

Figs. 7 and 8 has been drawn to observe the influence of the hydrostatic initial stress p on the distribution of the temperature θ and the strain field e against distance x for $\alpha = 0.5$, $\beta_0 = 0.1$ (i. e., fractional order generalized magneto-thermoelasticity) and these figures clearly indicate that the hydrostatic initial stress has an decreasing effect on both the temperature and strain fields within the region $0.0 \leq x \leq 3.5$ (approximately). It is also noticed that the magnitudes of both the temperature and strain fields are maximum for all the three cases (i.e., $p = 0.0, 0.2, 0.4$) at the boundary which is physically reasonable and then converge to zero gradually for large $x (\geq 3.5)$ which indicates a wave front. Finally, all curves for both the field variables θ and e approaches to zero for $x \geq 3.5$ (approximately) which is the location of wave front. From the mathematics view point, the non-Fourier thermal conduction equation is a damped wave equation, where the coefficient of θ represents the amount of damping. This is the difference between the Fourier and non-Fourier heat conduction. All the three curves predicting the distributions of θ and e have similar nature. The temperature distributions have non-zero values only in a bounded region of the half-space which is physically reasonable due to characteristics of finite wave speeds in generalized thermoelasticity.
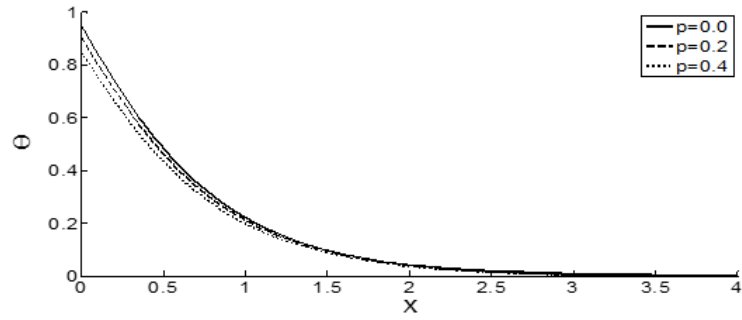
Fig. 7 – Temperature distribution for $\alpha = 0.5$.
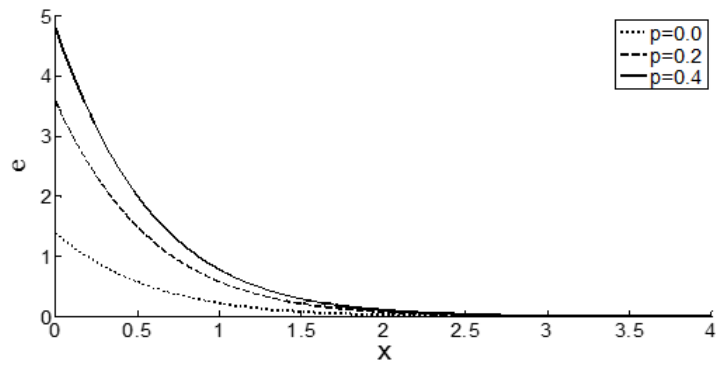
Fig. 8 – Distribution of the strain field for $\alpha = 0.5$.
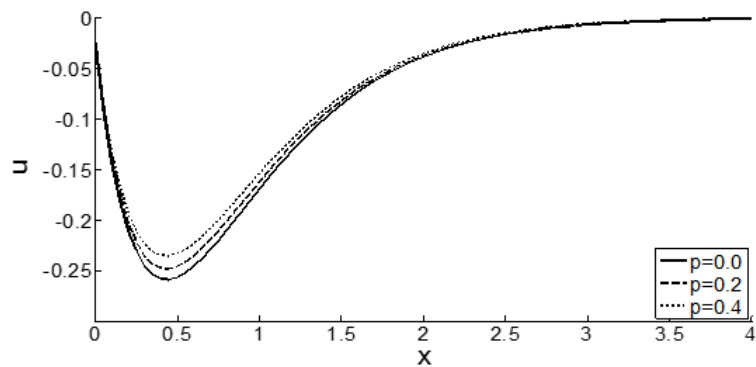
Fig. 9 – Horizontal displacement distribution for $\alpha = 0.5$.

33
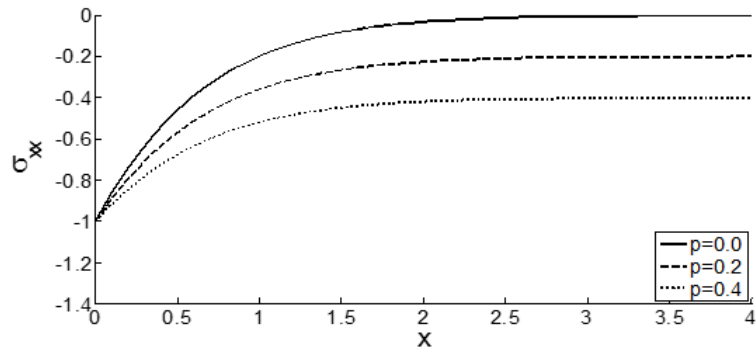
Fig. 10 – Distribution of the stress σ_{xx} for $\alpha = 0.5$.
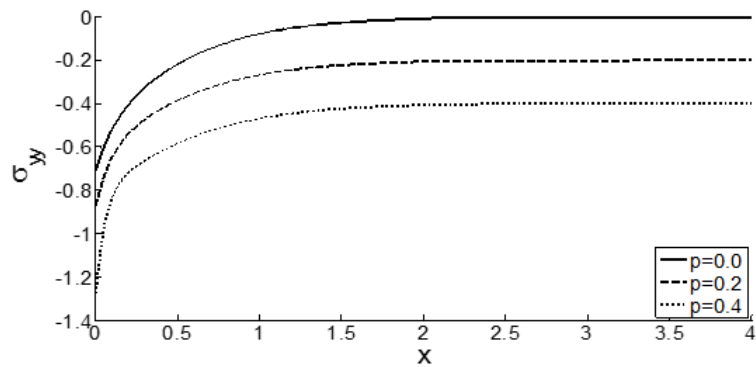
Fig. 11 – Distribution of the stress σ_{yy} for $\alpha = 0.5$.

Fig. 9 depicts the variation of horizontal displacement u at different positions of distance x $(0.0 \leq x \leq 4.0)$ for three different values of p, namely $p = 0.0, 0.2, 0.4$. It can be seen from the profile that the displacement u increases as the value of p increases and it exhibits negligible impact of the hydrostatic initial stress near the boundary of the half-space. It can also be seen that the maximum impact zone of hydrostatic initial stress p is around the location $x = 0.5$ and this impact dies out as we move away from the boundary. For all the three values of p, displacement field shows the same nature.

Fig. 10 and 11 exhibits the space variations of the normal stresses σ_{xx} and σ_{yy} with three different values of p for $\alpha = 0.5$, $\beta_0 = 0.1$. Fig. 10 indicates that when the thermally insulated boundary of the half-space is subjected to a normal load equal to $-p_0$ [Eq. (50)], σ_{xx} shows a negative value -1.0 at the boundary of the half-space for all values of $p = 0.0, 0.2, 0.4$ and then it is increasing inside $0.0 \leq x \leq 3.5$. After some distance from the boundary, it attains the constant values $0.0, 0.2$ and 0.4 respectively which leads to satisfy the solution (44). Fig. 11 shows that the stress field σ_{yy} starts with a negative value at the boundary and then starts to increase to reach its maximum values $0.0, 0.2$ and 0.4 respectively. It is interesting to note that the hydrostatic initial stress has an increasing effect on σ_{yy} near the boundary within $0.0 \leq x \leq 0.35$ (approximately) and then the factor

hydrostatic initial stress acts to decrease the value of σ_{yy} in the range $0.35 \leq x \leq 3.5$ (approximately). Finally this normal stress component converges to the negative values 0.0, 0.2, 0.4 due to the nature of the analytical solution (45). We can also notice from these figures that both the normal stress fields are compressive in nature and it shows negligible impact of the hydrostatic initial stress near the boundary of the half-space. So the maximum impact zone of the factor p is $0.35 \leq x \leq 3.5$ (approximately).
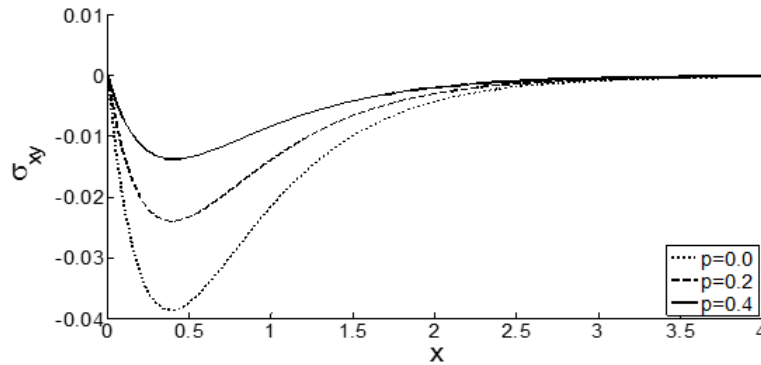
Fig. 12 – Distribution of the stress σ_{xy} for $\alpha = 0.5$.

Fig. 12 shows distribution of the shearing stress σ_{xy} with respect to distance x at three different values of p for $\alpha = 0.5$, $\beta_0 = 0.1$. We noticed that σ_{xy} takes zero value at the boundary which leads to satisfy the boundary conditions of the problem. All the three curves show similar trends i.e., starting with zero values then decreasing within the region $0.0 \leq x \leq 0.38$ and then increases to converge to zero value for $x \geq 0.38$. This type of nature has been seen due to nature of the boundary conditions. The parameter has an increasing effect on the distribution of the shearing stress σ_{xy}. Also the shearing stress σ_{xy} shows its compressive nature as expected.

8. Conclusions

The main goal of this study is to establish a new mathematical model of heat conduction with time fractional order for a homogeneous isotropic thermoelastic material which is placed in magnetic field with two-temperature under the influence of hydrostatic initial stress as an improvement and progress in the field of generalized thermoelasticity du to the fact that a thermoelastic model with a fractional heat conduction law can describe simply and elegantly the complex characteristics of a solid body. According to the above analysis, the following conclusions can be noted :

(i) Figs. 1-12 depicts that, all the physical quantities are restricted in a bounded region which is in accordance with the 'notion' of generalized thermoelasticity theory with fine wave speeds and supports the physical facts.

(ii) The fractional parameter has significant effect on all the studied field quantities.

(iii) According to the fractional parameter which describes the ability of thermoelastic material to conduct heat, various type of new classification of materials must be constructed

(iv) The effect of hydrostatic initial stress parameter on all the studied fields is very much significant.

(v) All the physical quantities satisfy the boundary conditions. Deformation of a body depends on the nature of the applied force as well as the type of boundary conditions.

(vi) Analytical solutions based upon normal mode analysis of the thermoelastic problem in solids have been developed and utilized.

(vii) From the temperature distributions, we have found wave type heat propagation with finite speeds in the medium.

(viii) The introduction of hydrostatic initial stress to the generalized magneto-thermoelastic half-space medium with a time-fractional heat conduction law provides a more realistic model for studying various types of problems in this field.

REFERENCES

[1] Ezzat, M. A., El Karamany, A. S., 2011. Fractional Order Heat Conduction Law in Magneto- Thermoelasticity involving Two Temperatures, Journal of Applied Mathematics and Physics 62, p. 937.

[2] Jumarie, G., 2010. Derivation And Solutions of Some Fractional Black Scholes Equations in Coarsegrained Space and Time, Application to Merton's Optimal Portfolio, Computers & Mathematics with Applications 59, p. 1142.

[3] Othman, M. I. A., Sarkar, N. and Atwa, S. Y., 2013. Effect of Fractional Parameter on Plane Waves of Generalized Magnetothermoelastic Diffusion with Reference Temperature-Dependent Elastic Medium, Computers & Mathematics with Applications 65, p. 1103.

[4] Abbas, I. A., 2014. A Problem on Functional Graded Material under Fractional Order Theory of Thermoelasticity, Theoretical and Applied Fracture Mechanics 74, p. 18.

[5] Youssef, H., Al-Lehaibi, E., 2010. Fractional Order Generalized Thermoelastic Half Space Subjected to Ramp Type Heating, Mechanics Research Communications 37, p. 448.

[6] Povstenko, Y. Z., 2005. Fractional Heat Conduction Equation and Associated Thermal Stress, Journal of Thermal Stresses 28, p. 83.

[7] Povstenko, Y. Z., 2009. Fractional Radial Diffusion in an Infinite Medium with Cylindrical Cavity, Quarterly of Applied Mathematics 67, p. 113.

[8] Bachher, M., Sarkar, N., Lahiri, A., 2014. Generalized Thermoelastic Infinite Medium with Voids Subjected to a Instantaneous Heat Sources with Fractional Derivative Heat Transfer, International Journal of Mechanical Sciences 89, p. 84.

[9] Bachher, M., Sarkar, N., Lahiri, A., 2015. Fractional Order Thermoelastic Interactions in an Infinite Porous Material Due to Distributed Time-Dependent Heat Sources, Meccanica 50, p. 2167.

[10] Sarkar, N., Lahiri, A., 2012. A Three-Dimensional Thermoelastic Problem for a Half-Space without Energy Dissipation, International Journal of Engineering Science 51, p. 310.

[11] Sarkar, N., 2014. Analysis of Magneto-Thermoelastic Response in a Fiber-Reinforced Elastic Solid Due to Hydrostatic Initial Stress and Gravity Field, Journal of Thermal Stresses 37, p. 1.

[12] Othman, M. I. A., Song, Y. Q., 2008. Effect of Rotation on Plane Waves of the Generalized Electromagneto-Thermo-Viscoelasticity with two Relaxation Times, Applied Mathematical Modelling 32, p. 811.

[13] Lord, H. W., Shulman, Y. A., 1967. Generalized Dynamical Theory of Thermoelasticity, Journal of the Mechanics and Physics of Solids 15, p. 299.

[14] Montanaro, A., 1999. On Singular Surface in Isotropic Linear Thermoelasticity with Initial Stress, Journal of the Acoustical Society of America 106, p. 1586.

[15] Youssef, H., 2006. Theory of Two-Temperature Generalized Thermoelasticity, IMA Journal of Applied Mathematics 71, p. 383.